

# Mobile Node Localization in Wireless Networks: Path-Loss Model, Trilateration, and Error Mitigation in a 5G Sub-6 GHz Scenario

Navid Heydarishahreza\*, Nirwan Ansari

Advanced Networking Laboratory, Department of Electrical and Computer Engineering, New Jersey Institute of Technology, Newark, NJ, 07102, USA.

\*Corresponding author

**In this paper, we proffer a novel technique designed for low-cost and computationally light localization of mobile nodes in an urban terrain, by leveraging the extended COST 231 Hata Path-Loss (PL) model and the Trilateration technique. Our approach accounts for the possibility of a Non-Line-of-Sight (NLoS) scenario in a medium-sized city, wherein one of the three reference nodes required for the trilateration approach encounters NLoS impediments. Our proposed method proceeds with localization by utilizing solely two Line-of-Sight (LoS) reference nodes, while integrating the localization system simulator with an Extended Kalman Filter (EKF). The simulation results presented herein demonstrate a marked enhancement in performance, surpassing that of trilateration in scenarios where three LoS nodes cannot be established.**

*Index Terms*—Wireless Networks, Trilateration, Localization, Path-Loss Models, Error Mitigation, 5G.

## I. INTRODUCTION

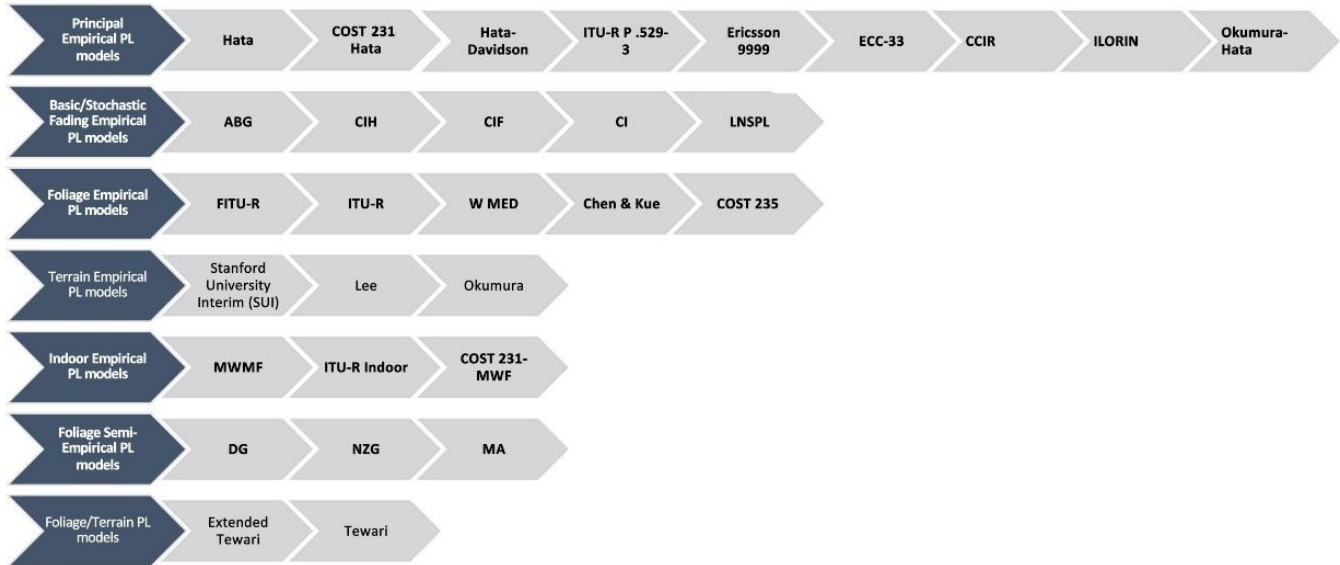
**L**OCALIZATION, defined as the process of estimating the orientation and position of a moving object, has already become an instrumental feature of the universal Smart-X applications [1], being studied since the emergence of wireless mobile technology. Numerous applications in our modern world benefit from location-aware communications, including Autonomous Driving, Industrial IoT (IIoT), and Tactile Internet. Wireless location-based systems are revolutionizing internet-based applications and remote physical interaction, evolving them into more sophisticated systems [2]. Over recent decades, various localization techniques have been proposed, utilizing visible light [3], ultrasound [4], inertial sensors [5], hybrid signals [6], and, specifically, Radio Frequency (RF) [7], which is our focus here. RF signals, as the omnipresent feature of current cellular networks, are immensely deployed for location estimation. Based on RF measurements, location determination techniques can be categorized into Angle of Arrival (AoA) [8], Time of Arrival (ToA) [9], and Received Signal Strength (RSS) [10]. ToA localization systems offer centimeter-level accuracy but require high precision time synchronization (nanosecond-level) between wireless reference nodes and mobile nodes, making them costly. AoA localization systems still necessitate specific hardware including a phase-detection mechanism. Besides, since this technique uses angles, error can start to rise as the distance between the reference and mobile node increases. Considering all these issues, the cost and the complexity of AoA and ToA location estimation solutions limit their feasibility in low-cost, unsophisticated applications. In contrast to ToA or AoA, the RSS technique is straightforward to implement and cost-effective. It is compatible with basic legacy consumer devices and can be applied to estimate distances using parametric

Path-Loss (PL) models. However, it provides relatively lower accuracy compared to ToA and AoA methods.

PL between a transmitter and a receiver is defined as the ratio of transmitted to received power, expressed in decibels, and includes all power losses as the radio wave propagates and interacts with obstacles, attenuating all the way. Wave propagation mechanisms are mainly associated with refraction, reflection, diffraction, and scattering, which can be discussed separately. PL models are mainly classified as empirical, stochastic, and deterministic. Empirical PL models are attained based on measurements and observations, under different ambient conditions, and can be tuned with measurements specific to any type of geographical area. They characterize wave propagation in terms of the distance between the receiver and transmitter, antenna heights and angles, operating frequency, walls and obstacles, etc. As reported in the literature, the path between the receiver and the transmitter can be either LoS or NLoS [11-13]. Numerous empirical PL models are available, including principal models such as Hata [14], COST 231 Hata [15], and Ericsson 9999 [16]. Table 1 summarizes the majority of famous empirical PL models in different environments and scenarios.

Among this extensive spectrum of empirical PL models, Hata stands out as the most widely adopted while COST 231 Hata, which represents one of the latest extensions to the Hata model, is practical for 5G networks. COST 231 Hata can be used in network planning of legacy networks and non-standalone deployments in 5G. It assumes environmental type parameters, offering simplicity and significantly expedited computation time. While COST 231 Hata works rather well in urban areas, its response may be slow when the environment changes rapidly. Besides, the transmitter antenna height must be higher than the receiver's, and it does not account for foliage. Although there are other more accurate PL models that can be used for 5G networks, they are often more complex than the COST 231 Hata model [15, 17]. Another criterion in localization methods, is protection against malicious attacks, which

TABLE I: Famous empirical PL models in different environments and scenarios [17].



can compromise the accuracy of mobile node localization. In NLoS scenarios, a non-malicious node behaves similarly to a malicious node [12].

Localization-based applications that prioritize energy efficiency and computational simplicity, such as battery-powered asset tracking, low-power IIoT, and energy-efficient wearables, require localization solutions that minimize both energy consumption and computational complexity. These applications are commonly deployed in urban environments, where NLoS reference nodes can introduce significant localization challenges. To tackle these challenges, we present an innovative RSS-based localization that harnesses the principles of the COST 231 Hata PL model. Our approach makes use of the low energy consumption of the RSS technique and the efficient computational capabilities offered by the COST 231 Hata PL model, effectively mitigating the inherent low accuracy limitations of RSS-based localization technique. This approach is ideally suited for location-based applications in medium-sized cities, especially when one of the three required reference nodes for trilateration, as depicted in Fig. 1, encounters NLoS conditions—a realistic and common occurrence. To further enhance accuracy and tackle additional challenges, such as dealing with a single NLoS reference node or adhering to the reference node antenna to be positioned higher than the mobile node according to the COST 231 Hata PL model as well as potential altitude variations in certain locations, we augment our solution by integrating COST 231 Hata PL model and Trilateration with the Kalman Filter (KF), a lightweight estimation algorithm. KF, a simple robust estimator, is often used to filter out rapid changes, noise, interference, and smooth the motion trajectory. In any dynamic system with uncertain information, KF can efficiently predict the next trend of the system [18-20]. Simulation results of our method demonstrate promising efficiency, making it applicable to a wide range of industrial applications. In Section II, we discuss our proposed localization system without KF to further examine the errors

our simulated system encounters. In Section III, we apply KF to mitigate these errors, and the numerical results are presented in Section IV to support a more comprehensive comparison. We finally conclude our work in Section IV.

## II. THE PROPOSED LOCALIZATION SYSTEM

Popular algorithms for RSS-based node localization are centroid, gradient, and trilateration. The centroid algorithm determines the mobile node’s location by calculating the average position of all reference nodes within the transmission range. Although it is easy to implement, this method exhibits relatively limited accuracy in localization. In contrast, the gradient algorithm utilizes the signal strength distribution in the surrounding area to estimate the mobile node’s direction. By combining multiple directional estimates, this algorithm ascertains the mobile node’s location. The gradient algorithm effectively addresses sampling bias and mitigates the impact of non-uniform signal propagation. However, it requires extensive RSS measurements to yield desirable results. Trilateration, as another approach, employs a PL model to convert RSS measurements into distances between the source node and receivers. These distances are then combined to determine the source node’s location. The trilateration algorithm depends on having access to PL model parameters, such as source transmitting power and PL exponent. Typically, these parameters are assumed to be known beforehand through a calibration phase. In trilateration, the three reference nodes’ positions  $(X_{R_1}, Y_{R_1})$ ,  $(X_{R_2}, Y_{R_2})$ ,  $(X_{R_3}, Y_{R_3})$ , and their respective distances  $d_1$ ,  $d_2$ ,  $d_3$  from the mobile node  $(X_M, Y_M)$  calculated by the COST 231 Hata PL model, are assumed known [19]. RSS-based ranging approaches translate an RSS from a mobile node to a specific reference node using a PL model or a propagation channel model. The majority of PL models are customizable by manipulating parameters, with respect to the environment [20]. Referring to the COST 231 Hata PL model [15], the

propagation loss which is the difference value between the received power and the radiated power, is calculated as

$$L_p(dB) = P_t - P_r. \quad (1)$$

and the standard formula for median propagation loss is obtained by

$$L_p(dB) = 46.3 + 33.93 \log_{10}(f_c) - 13.82 \log_{10}(h_b) - a(h_m) + (44.9 - 6.55 \log_{10}(h_b)) \log_{10}(d), \quad (2)$$

where  $f_c$  is the carrier frequency in the range 1.5-2GHz,  $h_b$  is the reference node height which is 30-200m,  $d$  is the distance between the mobile node and the reference node 1-20km, and  $a(h_m)$  is the correction factor for  $h_m$  (mobile node antenna height 1-10m), calculated as

$$a(h_m) = 3.2(\log_{10}(11.75h_m))^2 - 4.97 \quad (dB), \quad (3)$$

which is assumed zero in medium cities. The distance  $d$  can be calculated by

$$d(km) = 10^{\frac{L_p + 13.82 \log_{10}(h_b) - 33.93 \log_{10}(f_c) - 46.3 + a(h_m)}{44.9 - 6.55 \log_{10}(h_b)}}. \quad (4)$$

Hence, with the four parameters  $L_p$ ,  $f_c$ ,  $h_b$ , and  $a(h_m)$ , the distance between the reference node and the mobile node, forming a circular locus, can be determined. On the other hand, in trilateration, by knowing the coordinates of the three reference nodes  $(X_{R_1}, Y_{R_1})$ ,  $(X_{R_2}, Y_{R_2})$ ,  $(X_{R_3}, Y_{R_3})$  and their respective distances  $d_1$ ,  $d_2$ ,  $d_3$  from the mobile node (calculated using the COST 231 Hata PL model), the mobile node coordinates  $(X_M, Y_M)$  can be determined. This process involves solving a system of equations that includes three circle equations

$$\begin{cases} (X_{R_1} - X_M)^2 + (Y_{R_1} - Y_M)^2 = d_1^2 \\ (X_{R_2} - X_M)^2 + (Y_{R_2} - Y_M)^2 = d_2^2 \\ (X_{R_3} - X_M)^2 + (Y_{R_3} - Y_M)^2 = d_3^2 \end{cases}. \quad (5)$$

In this method, a minimum of three LoS reference nodes are required. Consider a scenario in which the mobile node is a user situated in an urban terrain characterized by the presence of foliage and tall buildings. It is highly probable that, in such a typical environment, at least one of the three required reference nodes for trilateration technique encounters NLoS conditions. In this particular scenario, our low-energy location-based application faces a significant challenge. Moreover, due to the error associated with the COST 231 Hata PL model and the attenuation mechanisms, a considerable location estimation error arises earlier on. Even with the COST 231 Hata model parameters, we can still estimate the mobile node's location using only two LoS reference nodes, using (5), albeit with a larger error. As shown in Fig. 1, when only the two LoS reference nodes, labeled as 1 and 2, are available, the distances from these two LoS reference nodes ( $d_1$  and  $d_2$ ) can be calculated using the first two equations in (5). The intersections of the two green circles, derived from (5) and represented by coordinates  $(X_{R_1}, Y_{R_1})$ ,  $(X_{R_2}, Y_{R_2})$ , are approximate locations for the mobile node which could be either A or B. The antenna sectors of the reference nodes can be instrumental in determining the true location of the mobile node. By measuring the signal strength and direction from

antenna sectors, we can determine that the mobile node is most likely located in close proximity to point A in this scenario. Therefore, the mobile node's position is approximated as point A (the gray point), although this approximation comes with a larger error compared to having three LoS reference nodes. In [20], using a single reference node and the COST 231 Hata model in an urban area, the mean estimation error of a mobile node localization was obtained in the range 184-207m, with more than 95% of all measurements resulting in a localization error under 679m. In the next section, we present the simulated localization errors when using 2 LoS reference nodes, admitting that as more reference nodes go NLoS, the localization error increases.

### III. ERROR MITIGATION BY KALMAN FILTERING

KF is capable of predicting the next state of a system, by using the current and previous states. It is defined by one equation with two phases: prediction and update. KFs are used to estimate system parameters and minimize noise error, well suited for dynamic systems. In our localization scenario, we have a non-linear equation (4) that is not compatible with the simple KF. Instead, we use the Extended Kalman Filter (EKF), which is the non-linear version of KF. Our proposed localization system is realized according to the block diagram shown in Fig. 2. We use MATLAB R2022b in Block 1 to design a simulator that generates noisy PLs  $L_{p_1-Noisey}$  and  $L_{p_2-Noisey}$  with respect to the reference nodes 1 and 2, and the mobile node. For the simulation, we assume that the coordinates of reference nodes 1 and 2 are  $(X_{R_1}, Y_{R_1})=(2, -1)$ ,  $(X_{R_2}, Y_{R_2})=(-2, 3)$ , respectively, and the initial coordinates of the mobile node are  $(X_M, Y_M) = (3, 1)$ , all in kilometers. In addition, we adopt the following state-space mobility model for the mobile node:

$$\begin{cases} X = \begin{bmatrix} X_M \\ Y_M \\ \dot{X}_M \\ \dot{Y}_M \end{bmatrix}, & \dot{X} = \begin{bmatrix} 1 & 0 & dt & 0 \\ 0 & 1 & 0 & dt \\ 0 & 0 & 1 & 0 \\ 0 & 0 & 0 & 1 \end{bmatrix} X, \\ Y = \begin{bmatrix} d_1 \\ d_2 \end{bmatrix} = \begin{bmatrix} \sqrt{(X_{R_1} - X_M)^2 + (Y_{R_1} - Y_M)^2} \\ \sqrt{(X_{R_2} - X_M)^2 + (Y_{R_2} - Y_M)^2} \end{bmatrix} \end{cases} \quad (6)$$

Here,  $\dot{X}_M$ ,  $\dot{Y}_M$  are the mobile node speed in km/s, with respect to the horizontal and vertical axes of a 2-D Cartesian space and assumed to be  $\dot{X}_M = 0.01 \text{ km/s}$ ,  $\dot{Y}_M = 0.015 \text{ km/s}$ . Having  $d_1$ ,  $d_2$ , and (2), (3), with system parameters  $f_c=2\text{GHz}$ ,  $h_b=70\text{m}$ ,  $h_m=1.5\text{m}$ , the PLs  $L_{p_1}$  and  $L_{p_2}$  can be calculated. White Gaussian Noise with a signal-to-noise ratio of 33 decibels is then added. The simulated PL values (output of Block 1) relative to the mobile node and the two LoS reference nodes, with a sampling interval of 0.25s, are obtained as shown in Fig. 3. As input to Block 1, we have the actual  $X_M$  and  $Y_M$  based on the mobility model (6), which are changing over time. The outputs of Blocks 3 and 4 represent the outputs of the localization system without and with EKF, respectively.

Having the above PLs, the PL exponent is estimated to be 3.28. Block 2 takes the simulated  $L_{p_1-Noisey}$  and  $L_{p_2-Noisey}$  as

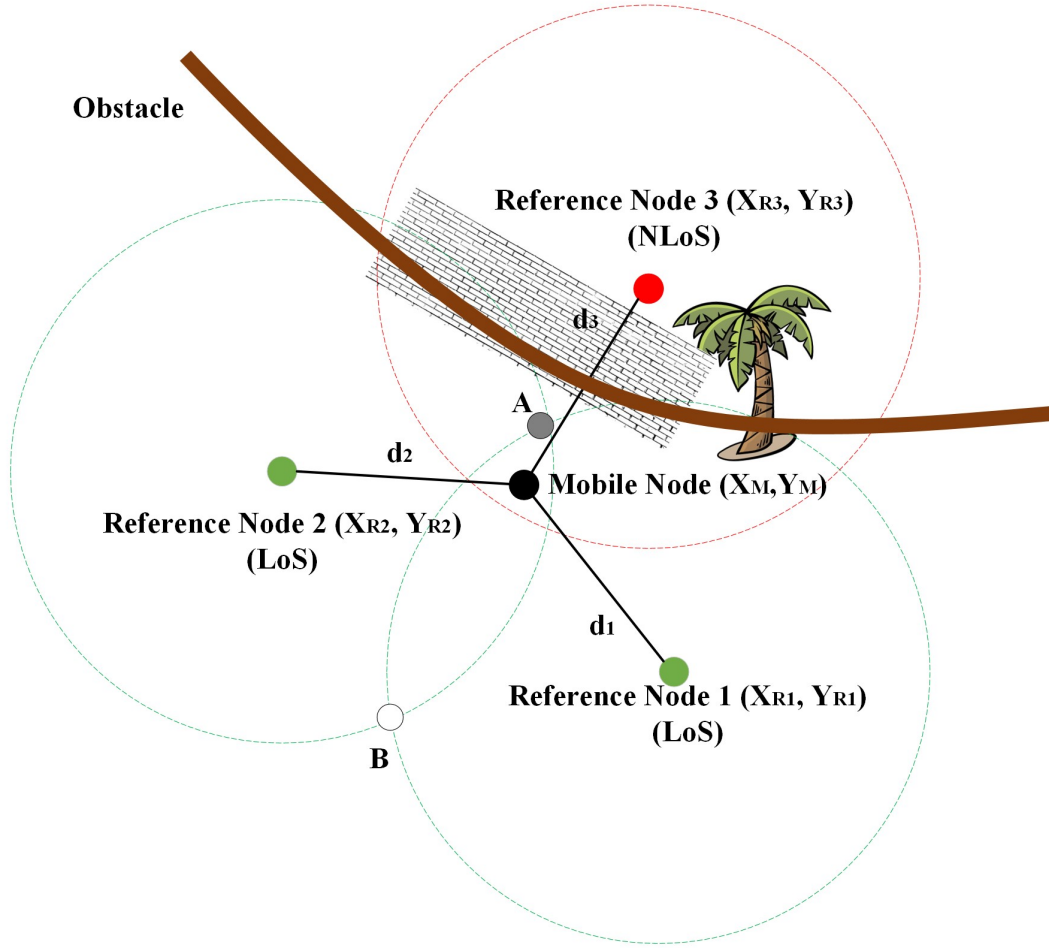


Fig. 1: Trilateration method, 2 LoS and 1 NLoS reference nodes.

input and uses (4) to calculate the relative simulated distances as shown in Fig. 4. Block 3 uses  $\tilde{d}_1$ ,  $\tilde{d}_2$  along with (5), to intersect the two circles with respective radii and calculate the estimated location of the mobile node ( $\tilde{X}_M$ ,  $\tilde{Y}_M$ ). Expanding (5) for the first two circles and rearranging the terms in each equation, then subtracting the second equation from the first to omit  $\tilde{X}_M$ , and  $\tilde{Y}_M$  will offer:

$$2(X_{R1} - X_{R2})\tilde{X}_M = (X_{R1}^2 - X_{R2}^2) + (Y_{R1}^2 - Y_{R2}^2) - (\tilde{d}_1^2 - \tilde{d}_2^2) \quad (7)$$

$$2(Y_{R1} - Y_{R2})\tilde{Y}_M = (X_{R1}^2 - X_{R2}^2) + (Y_{R1}^2 - Y_{R2}^2) - (\tilde{d}_1^2 - \tilde{d}_2^2) \quad (8)$$

Solving (7) and (8) for  $\tilde{X}_M$ ,  $\tilde{Y}_M$ :

$$\begin{cases} \tilde{X}_M = \frac{(X_{R1}^2 - X_{R2}^2) + (Y_{R1}^2 - Y_{R2}^2) - (\tilde{d}_1^2 - \tilde{d}_2^2)}{2(X_{R1} - X_{R2})} \\ \tilde{Y}_M = \frac{(X_{R1}^2 - X_{R2}^2) + (Y_{R1}^2 - Y_{R2}^2) - (\tilde{d}_1^2 - \tilde{d}_2^2)}{2(Y_{R1} - Y_{R2})} \end{cases} \quad (9)$$

Solving (9) for  $\tilde{X}_M$ ,  $\tilde{Y}_M$  yields two points, A, and B as shown in Fig. 1. Logically, the mobile user should be either at point A or B. The reference nodes use sector antennas capable of detecting signals within their specific service areas.

After evaluating the received signals from the mobile node, the direction or angle of the received signal is determined. This information now can be leveraged to pinpoint the true location of the mobile node, which is point A. Now the output of the proposed system in Block 3 is the location of the mobile node estimated by the COST 231 Hata model and 2 LoS reference nodes. In Block 4, the EKF kicks in to smooth the estimated trajectory. The EKF takes simulated observations  $\tilde{d}_1$  and  $\tilde{d}_2$  which are calculated using the COST 231 Hata model and generated in the output of Block 2, and simulated measurements  $\tilde{X}_M$ ,  $\tilde{Y}_M$  calculated in Block 3 by intersecting the first two circle equations in (5). Block 3 serves as a data source or a sensor. In the output of Block 4, the EKF provides simulated estimated measurements denoted as  $\hat{d}_1$ ,  $\hat{d}_2$ . Following a similar procedure to that in Block 3, we obtain the estimated coordinates  $\hat{X}_M$ ,  $\hat{Y}_M$ . In the EKF algorithm, the measurement noise covariance matrix is set to 1. The *a priori* estimation  $X_{t+1|t}$  predicts the state in the next time sample, while the *a posteriori* estimation  $X_{t|t}$  is accomplished by utilizing both observed measurements  $\hat{d}_1$ ,  $\hat{d}_2$  and the *a priori* estimation at the previous sampling time  $X_{t|t-1}$ . The covariance of  $X_{t+1|t}$  is calculated in each iteration, having an initial value of 1. As shown in Fig. 2, we have all the three types of location determined by now: the actual location of the

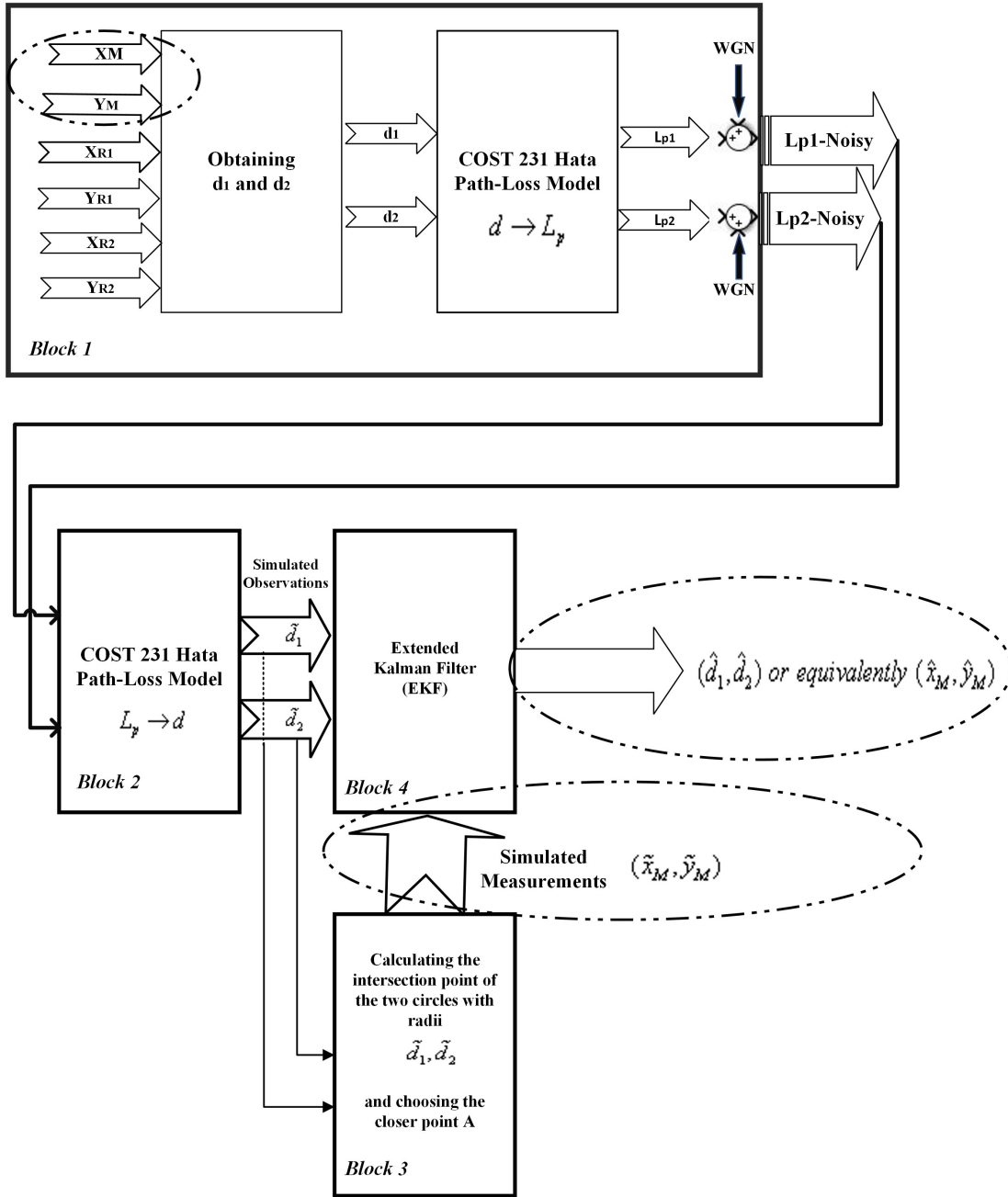


Fig. 2: Block diagram of the proposed localization system.

mobile node in all sampling times, the location determined by the COST 231 Hata PL model, and the location estimated by EKF (Fig. 5).

#### IV. NUMERICAL RESULTS

We adopt root mean squared error (RMSE) to benchmark the accuracy of the estimated positions of the mobile node movement for the first 300 seconds by the COST 231 Hata PL model and COST 231 Hata PL model with EKF, respectively, as shown in Fig. 6. Note that the RMSE for location estimation by the COST 231 Hata model is rising from about 10m in the first seconds of mobile node movement to more than 30m

in the last seconds of the sampling interval, while the EKF leveraged simulator starts with the RMSE of about 10m and ends up with the RMSE almost equal to 2m. The reason for this is that, despite the rational initial location estimation offered by COST 231 Hata, its performance gradually starts to exacerbate with the mobile node receding. The COST 231 Hata is deterministic, meaning that it assumes no measurement uncertainty. Thus, it is obvious that as the mobile node moves, the measurements deteriorate and the RMSE of COST 231 Hata is elevated. On the flip side, our EKF-based simulator showcases a noteworthy aptitude to optimize the estimated locations during the sampling time intervals. The EKF, a recursive algorithm, is intrinsically probabilistic, considering the

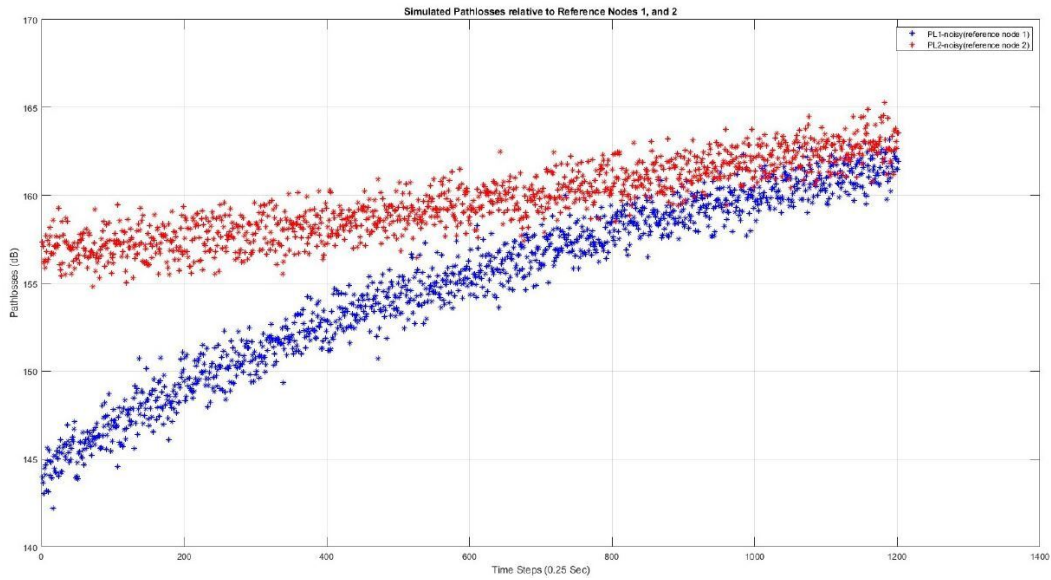


Fig. 3: Outputs of Block 1; Simulated Noisy PLs.

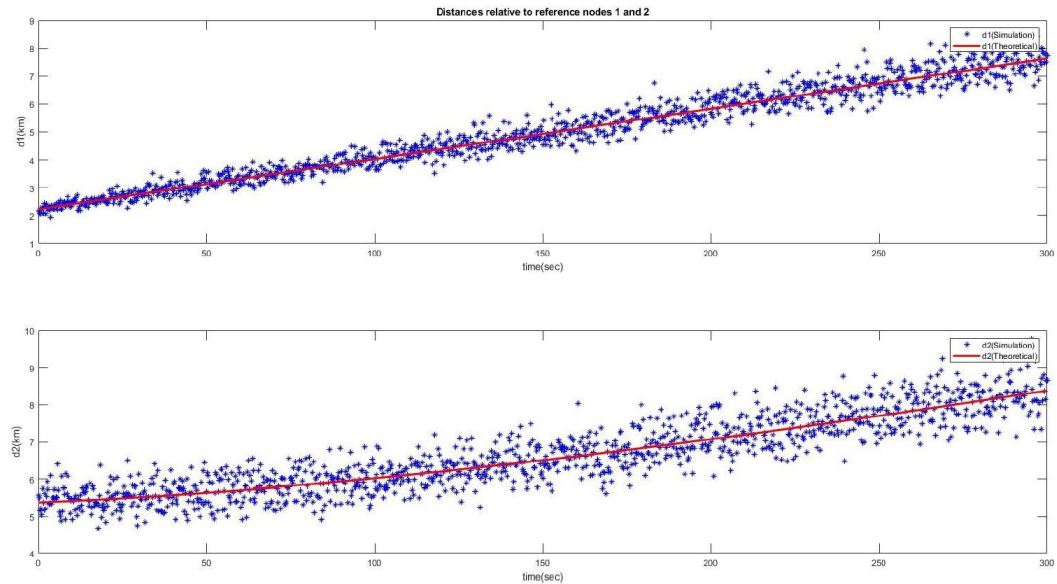


Fig. 4: Outputs of Block 2; Simulated  $d_1$  and  $d_2$ .

uncertainties of measurements. It continuously fine-tunes its location estimation by accepting new measurements, leading to a robust RMSE reduction. Considering error mitigation in localization for energy-efficient and computationally light applications, such as low-power wearables, IIoT, and asset tracking, it is essential to explore alternatives to EKF. One such alternative is Machine Learning (ML). The advantages of EKF over ML include efficient real-time performance, the utilization of prior knowledge for improved accuracy, sensor fusion capacities, and a transparent framework that facilitates error correction and diagnosis. These merits not only bolster performance but also contribute to cost-effectiveness, making EKF a practical choice for applications prioritizing computational simplicity and low energy consumption. EKF strikes a balance between accuracy and computational simplicity when

compared to resource-intensive ML approaches.

In urban environment with buildings and obstacles, the occurrence of shadowing phenomena is inevitable. To make the scenario more realistic, we introduced shadowing in the MATLAB simulations by incorporating strong white Gaussian noise into the pathlosses at each sampling time step. The RMSE results in Fig. 6 demonstrate the EKF’s ability in addressing challenges, including shadowing, and validating practical efficiency in real-world applications.

## V. CONCLUSION

We have developed a simulator for accurately achieving low-power and computationally light localization of mobile nodes in wireless networks, utilizing only 2 LoS reference nodes.

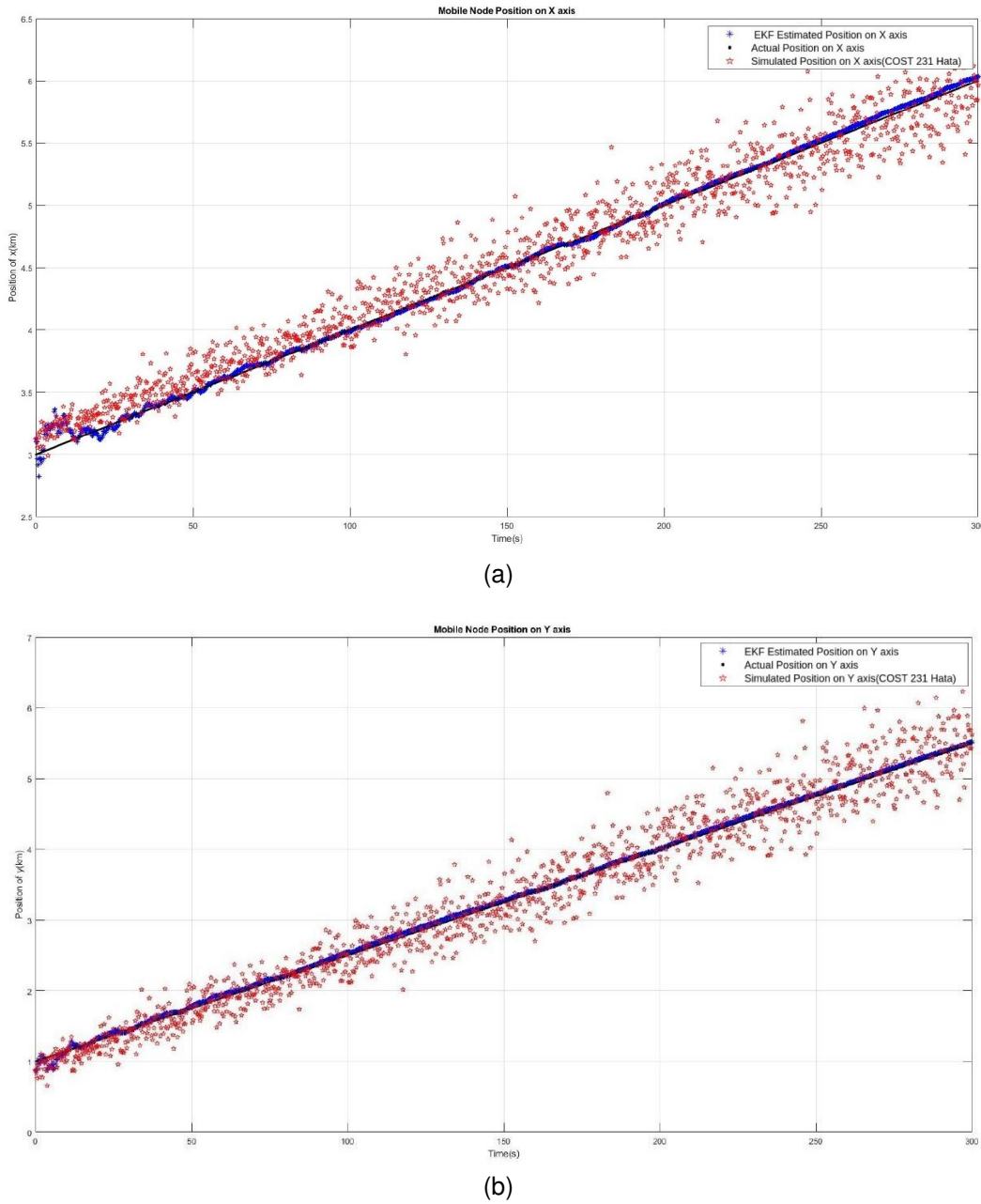


Fig. 5: The actual location of the mobile node at all sampling times, the location determined by the COST 231 Hata model, and the location estimated by EKF: (a) X-axis, and (b) Y-axis.

By leveraging trilateration with the COST 231 Hata Path-Loss model and the Extended Kalman Filter, we are able to reduce the RMSE from approximately 30 meters for the standalone COST 231 Hata model simulator, to just 2 meters for our proposed trajectory positioning model. These results clearly demonstrate the effectiveness of our approach in enhancing the reliability and accuracy of localization by utilizing readily available RSS data in wireless networks.

REFERENCES

[1] De Lima, Carlos, et al. "Convergent communication, sensing and localization in 6G systems: An overview of technologies, opportunities and

challenges." *IEEE Access*, vol. 9, 26902-26925, 2021.  
 [2] H. Chen, H. Srieddeen, T. Ballal, H. Wymeersch, M. -S. Alouini and T. Y. Al-Naffouri, "A Tutorial on Terahertz-Band Localization for 6G Communication Systems," *IEEE Communications Surveys and Tutorials*, vol. 24, no. 3, pp. 1780-1815, third quarter 2022.  
 [3] X. Guo, S. Shao, N. Ansari, and A. Khreishah, "Indoor Localization Using Visible Light via Fusion of Multiple Classifiers," *IEEE Photonics Journal*, vol. 9, no. 6, pp. 1-16, Dec. 2017  
 [4] Gabbrielli, Andrea, et al. "An echo suppression delay estimator for angle-of-arrival ultrasonic indoor localization." *IEEE Transactions on Instrumentation and Measurement*, vol. 70, pp. 1-12, 2021.  
 [5] Z. Karimi, M. Soheili, N. Heydarishahreza, S. Ebadollahi and B. Gill, "Smartphone Mode Detection for Positioning using Inertial Sensor, *IEEE 12th Annual Information Technology, Electronics and Mobile Communication Conference (IEMCON), Vancouver, BC, Canada*, pp. 0209-0215, 2021.  
 [6] X. Guo, N. Ansari, L. Li, and L. Duan, "A Hybrid Positioning System

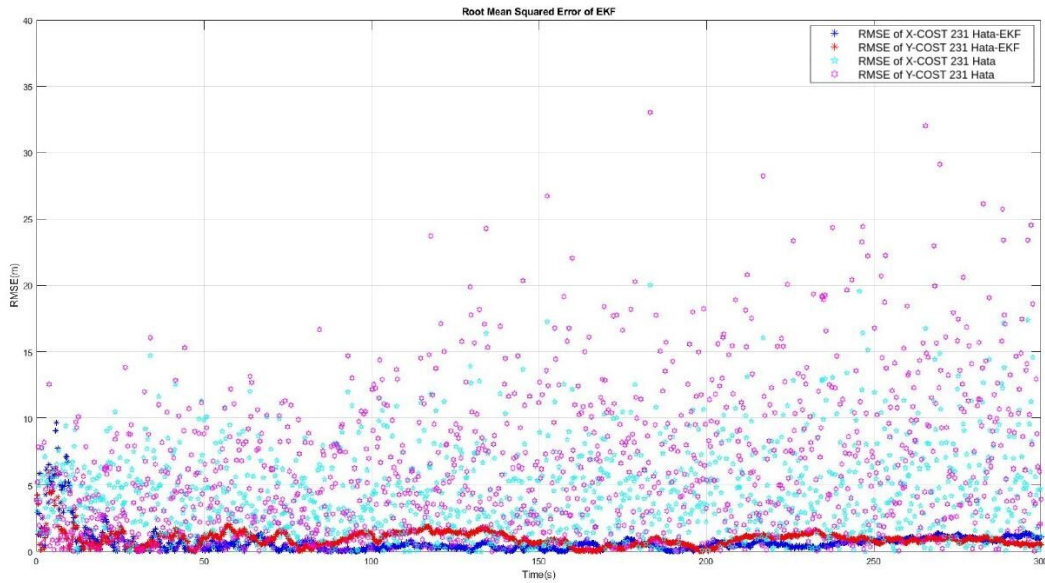


Fig. 6: RMSEs of the COST 231 Hata model itself, and our leveraged EKF system compared to mobile node actual locations.

for Location-based Services: Design and Implementation,” *IEEE Communications Magazine*, vol. 58, no. 5, May 2020.

[7] H. Wymeersch, J. He, B. Denis, A. Clemente and M. Juntti, “Radio Localization and Mapping With Reconfigurable Intelligent Surfaces: Challenges, Opportunities, and Research Directions,” *IEEE Vehicular Technology Magazine*, vol. 15, no. 4, pp. 52-61, Dec. 2020.

[8] Wang, Shengchu, Xianbo Jiang, and Henk Wymeersch. “Cooperative localization in wireless sensor networks with AOA measurements.” *IEEE Transactions on Wireless Communications*, vol. 21, no .8, pp. 6760-6773, 2022.

[9] H. Chen, G. Wang, and N. Ansari, “Improved Robust TOA-Based Localization via NLOS Balancing Parameter Estimation,” *IEEE Trans. Vehicular Technology*, vol. 68, no. 6, pp. 6177-6181, June 2019.

[10] X. Guo, R. Nkrow, N. Ansari, L. Li, and L. Wang, “Robust WiFi Localization by Fusing Derivative Fingerprints of RSS and Multiple Classifiers,” *IEEE Trans. Industrial Informatics*, vol. 16, no. 5, pp. 3177-3186, May 2020.

[11] Y. Li, X. Xie, and Y. Fang, “Cost-effective localization using RSS from single wireless access point,” *IEEE Trans. Instrum. Meas.*, vol. 69, no. 5, pp. 1860-1870, May 2020.

[12] B. Mukhopadhyay, S. Srirangarajan and S. Kar, “RSS-Based Localization in the Presence of Malicious Nodes in Sensor Networks,” *IEEE Transactions on Instrumentation and Measurement*, vol. 70, pp. 1-16, 2021.

[13] M. E. Diago-Mosquera, A. Aragón-Zavala, and G. Castañón, “Bringing it indoors: A review of narrowband radio propagation modeling for enclosed spaces,” *IEEE Access*, vol. 8, pp. 103875-103899, 2020.

[14] M. Hata, “Empirical formula for propagation loss in land mobile radio services,” *IEEE Trans. Veh. Technol.*, vol. 29, no. 3, pp. 317-325, Aug. 1980

[15] European Commission, Directorate-General for the Information Society and Media, “COST Action 231: Digital mobile radio towards future generation systems: Final Report,” *European Commission*, 1999.

[16] P. Begovic, N. Behlilovic and E. Avdic, “Applicability evaluation of Okumura, Ericsson 9999 and winner propagation models for coverage planning in 3.5 GHZ WiMAX systems,” *2012 19th International Conference on Systems, Signals and Image Processing (IWSSIP)*, Vienna, Austria, pp. 256-260, 2012.

[17] H. A. H. Alobaidy, M. N. Al-Dhief, M. T. Alresheedi, and N. N. Qasem, “Wireless transmissions, propagation and channel modelling for IoT technologies: Applications and challenges,” *IEEE Access*, vol. 10, pp. 24095-24131, 2022.

[18] H. Zheng, X. Zhong, and P. Liu, “RSS-based indoor passive localization using clustering and filtering in an LTE network,” in *2020 IEEE 91st Vehicular Technology Conference (VTC2020-Spring)*, Antwerp, Belgium, pp. 1-6, 2020.

[19] Y. Xu, J. Zhou, and P. Zhang, “RSS-based source localization when path-loss model parameters are unknown,” *IEEE Communications Letters*, vol. 18, no. 6, pp. 1055-1058, 2014.

[20] T. Janssen, R. Berkvens, and M. Weyn, “RSS-Based Localization and Mobility Evaluation Using a Single NB-IoT Cell,” *Sensors*, vol. 20, no. 21, pp. 6172, Oct. 2020.